Turkish Journal of Electrical Engineering & Computer Sciences

http://journals.tubitak.gov.tr/elektrik/

Research Article

Turk J Elec Eng & Comp Sci
(2021) 29: 897 – 912

doi:10.3906/elk-2004-132

Design of a compact wearable ultrawideband MIMO antenna with improved port isolation

Amit Baran DEY*, **Utkarsh BHATT**, **Wasim ARIF**
Department of Electronics and Communications Engineering, National Institute of Technology Silchar, Assam, India

Received: 19.04.2020 • **Accepted/Published Online:** 26.10.2020 • **Final Version:** 30.03.2021

Abstract: This study presents a compact dual element wearable ultrawideband (UWB) multi-in multi-out (MIMO) antenna with increased port isolation. The suggested design consists of a jeans substrate in which a tree-fashioned stub comprising of eight branches is introduced in the middle position of the partially etched antenna ground for improving the characteristics of port isolation. The proposed design occupies the frequency spectrum operating from 1.71 to 12.63 GHz (impedance bandwidth of around 152.3%) and satisfies the bandwidth demands for WiMAX (3.2–3.8 GHz), WLAN (5.15–5.35/5.72–4.85 GHz), the C Downlink-uplink bands (3.7–4.2/5.9–6.425GHz), ITU bands (8–8.5GHz) and the downlink defense band (7.2–7.5GHz). The antenna is able to maintain isolation between the ports $>$22dB across the entire UWB frequency spectrum. The coefficient of the envelope correlation for the whole operating band was observed to be $<$0.012 along with a very high diversity gain $>$9.9. The channel power loss of the proposed wearable UWB MIMO antenna is found to be $<$0.27 bit/s/Hz. The suggested UWB MIMO antenna, fascinated with optimization, covers an area of 35 $\times$ 35 mm^2. The suggested design is also able to perform satisfactorily when attached on-body. Simulation and testing fairly identified the performance of the antenna and rendered it to be an upstanding choice for wearable UWB applications.

Key words: Wearable antennas, diversity gain, multi-in-multi-out, total active reflection coefficient, ultrawideband spectrum

1. Introduction

Extensive demand for high-performance compact and wireless network antennas has increased in the last decade. The design of these mobile antennas has broad use in the fields of safety protection, emergency response, medical care, and assistance and athletic training [1]. Due to the increased data rate, the recent antenna system requires multiple antenna elements to accommodate increased functionality for multiple frequency applications. On the contrary, the recent wireless communication system needs to provide miniaturization along with multiple antenna elements [2]. Henceforth, the researchers should take care during the initial design paradigm. Ultrawideband (UWB) technology is progressively fetching importance due to the high level of data transmission in the broadband frequency spectrum at quite low power level. From this point of view, the ultrawideband MIMO finds it to be applicable for low power devices, providing extraordinary high data rates and excluding interference [3].

Wide bandwidth is often a crucial condition to maintain reliable efficiency, while the antenna is mounted on a particular human being [4]. A major change in the resonant band was observed due to antenna structural

*Correspondence: amitnitsece17@gmail.com

deformation [5]. In the past few years, also the development of wearable and lightweight MIMO antennas has been receiving attention [6, 7]. In lieu of its closeness to the human body and tissue loss at high permittivity medium, the design becomes difficult [6]. Additionally, the effects of the electromagnetic coupling within the wearable MIMO antenna and the human tissue are to be taken into account and potential long-term effects should also be noted [7].In comparison to this, multipath fading happens owing to various body postures and gestures. As a consequence, to boost the efficiency of signal transmission in wearable devices, multiple input multiple output (MIMO) antennas draw a great deal of interest from researchers. Therefore, during design of wearable textile antennas, special precautions should be addressed [8–11].

Different real-life circumstances are probably possible for wearable antenna systems, such as folding, bending, twisting washing etc., which may degrade the antenna performance [12]. Normally, surface wave losses were minimized in antennas made of textiles. This increases the antenna impedance bandwidth owing to the very low dielectric constant [13]. Numerous methods have been introduced to enhance the overall MIMO antenna performance such as introduction of defected ground structures (DGS), split ring resonators (SRR's), EBG structures, using reflectors, metamaterials, stubs, slots, broaden bandwidth, reduction in mutual coupling, using hexagonal rings [3, 14–21] etc.

MIMO antennas can also be used to increase the transmission capability and can also improve the spectral efficiency. It can also be used to simplify multiaccess layers and also to reduce air interference [22]. Because of the presence of multiple antenna elements, the mutual coupling that occurs in the MIMO system design should be reduced as far as possible [23]. The coupling can be reduced by increasing the distance between the antenna elements in the overall design. Nevertheless, the compactness of the structure is disturbed by this methodology. Hence, port decoupling or port isolation measures are therefore used instead of increasing the separation among elements so that high insulation is incorporated without negotiation in the compact design [24].

There is very little literature accessible on wearable MIMO antenna systems. Several wearable MIMO antennas are reported in the literature with higher port isolation [6, 7, 12, 25, 26]. A lightweight, single-layer fabric MIMO antenna is suggested for wearable applications in [6]. The antenna possesses good port isolation of 12 dB but the antenna gains drop to 1.6 dB and 1.2 dB due to human body loading. An optimized substrate integrated technology based dual-band textile MIMO antenna was proposed in [7] to achieve port isolation of -18dB and -35dB respectively in the lower and upper frequency bands. A wireless MIMO antenna is suggested in [27] for the WLAN applications. The antenna utilizes ground radiation with the properties of polarization diversity. The article presents 20 dB port isolation with a small 140 MHz bandwidth. The performance of a novel wearable MIMO antenna consisting of electro-textile antennas distributed at various human locations is analyzed in reference [25]. A wearable device dual band MIMO antenna to support 5G radio frequency has been presented in [26] operating from 3.3GHz to 3.6GHz and from 4.5GHz to 5GHz respectively. The extreme port isolation in this paper is approximately 17dB.

In this study, a new technique for reducing mutual coupling between the dual ports of UWB MIMO antenna is presented. The antenna's engineering methodology comprises of a partially etched ground plane connected with a tree shaped stub comprising of 8-branches. At first, the antenna size is miniaturized such that it can be conveniently combined with lightweight on-body gadgets. Thereafter, a broad bandwidth ranging from 1.45GHz to 12.02GHz is reached with the aid of adjusted size of the ground plane. It makes the antenna resilient to survive the detuning of the frequency. Eventually, two antenna components are used to build the MIMO system to enhance signal transmission efficiency. The suggested design ensures the wide band from 1.71

to 12.63GHz (S11 <-10 dB) frequency range covering the entire UWB bandwidth. We find envelope correlation coefficient (value <0.012) and diversity gain (value >9.9) to be very good from antenna analysis. The estimated bandwidth loss of the channel (value <0.27 bit/s/Hz) is also very small. During the study of our suggested model, we found port isolation to be very high (value >22dB) and a good stable radiation pattern across the full UWB frequency range. The design is modeled, evaluated, and configured by using Ansys HFSS[1]. A strong resemblance is found in the performance of the simulated and measured tests of the fabricated sample.

The remainder of the paper is described as follows. Section 2 deals with the entire antenna design process. Section 3 addresses the simulated and calculated effects together with antenna properties and a brief interpretation is given in Section 4.

2. The configuration and design of the antenna

The Figures 1a, 1b, and Figures 2a, 2b, 3a and 3b respectively depicts the envisioned design of the single and dual-element ultra-wideband MIMO antenna from the top and bottom perspective. The suggested UWB MIMO antenna has two rectangular-shaped patch components mounted atop the substrate. An inexpensive ready-for-use jeans with a relative dielectric constant of 2 having a tangent loss of 0.02 and a height of 1.59 mm is used as a substrate for the UWB MIMO antenna design. The relative parameters for jeans was checked on the jeans substrate for two simple printable samples in practical model and measurement [29]. The MIMO dual element antenna without the ground plane stub is also developed to test experimentally. Figures 4, 5, 6 depicts the three assembled models from their top and bottom perspective. The ports of the antenna are connected to 50Ω SMA connectors for exciting the antenna components.

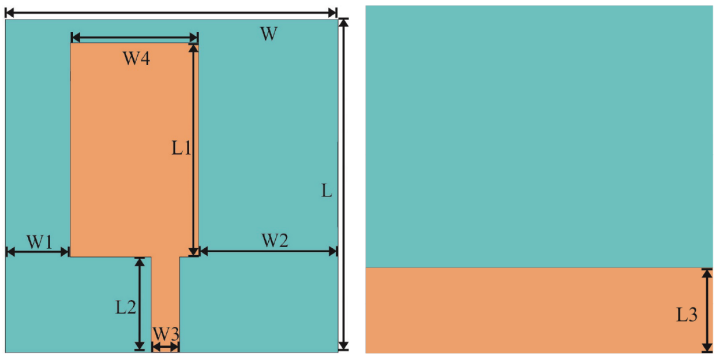

Figure 1. Single element UWB antenna configuration with partial ground plane (a) upper view representing rectangular shaped radiator (b) bottom view representing partially etched ground.

In the following subsections, measured results and antenna performance together with simulation results are addressed. The bottom layers of the suggested UWB MIMO antenna are shown in the Figures 1b, 2b, and 3b, respectively when the stub is removed and when the stub is inserted. The upper view of the dual-element antenna represents the antenna's two feeding components. The rear view of the UWB MIMO antenna with a novel tree-shaped isolator shows the modified structure of the ground plane. The antenna components are positioned at a distance of approx. 3.2 mm. The main purpose of instituting the tree shaped stub comprising 8-branches in the middle of the ground plane is to improve mutual decoupling within the ports. The dimensional constraints of the suggested UWB MIMO design are outlined by Table 1.

[1]Ansys HF. Ansoft Corp., Pittsburgh, PA ver. 19.

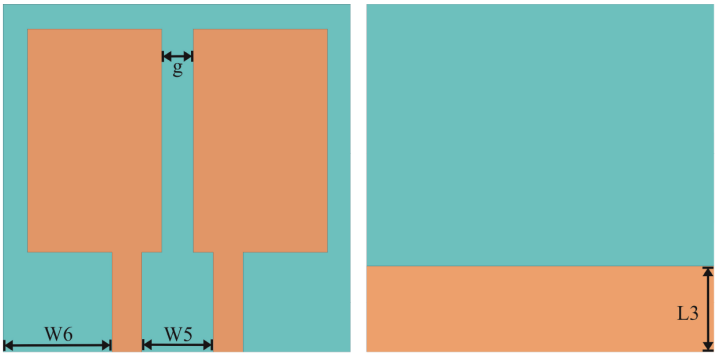

(a) (b)

Figure 2. Dual element UWB MIMO antenna configuration with no isolator (a) upper view of the MIMO antenna with two rectangular radiators (b) bottom view of the MIMO antenna with partial ground plane.

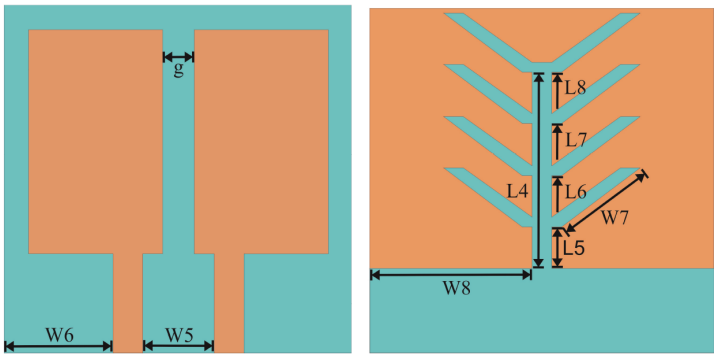

(a) (b)

Figure 3. Dual element UWB MIMO antenna configuration with an isolator (a) upper view of the MIMO antenna with two rectangular radiators (b) bottom view of the MIMO antenna with tree-shaped isolator having 8 branches attached to GP.

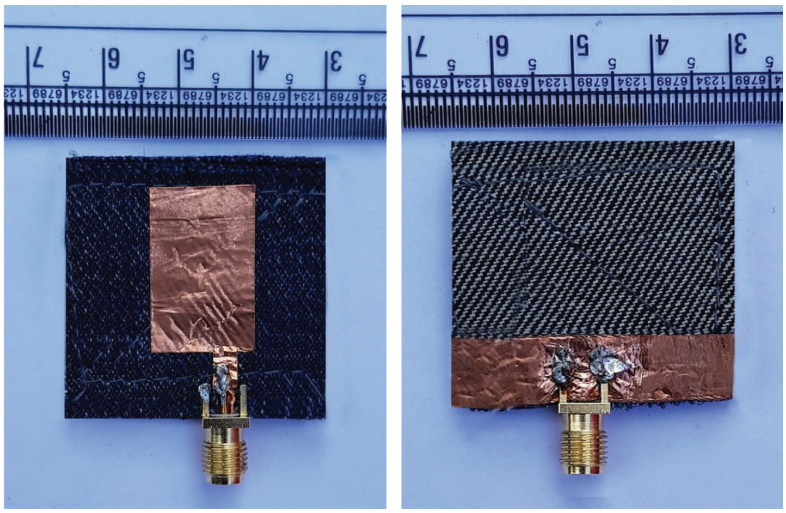

(a) (b)

Figure 4. Fabricated prototype of (a) upper portion of antenna with single element. (b) bottom portion of single element antenna with partial ground plane.

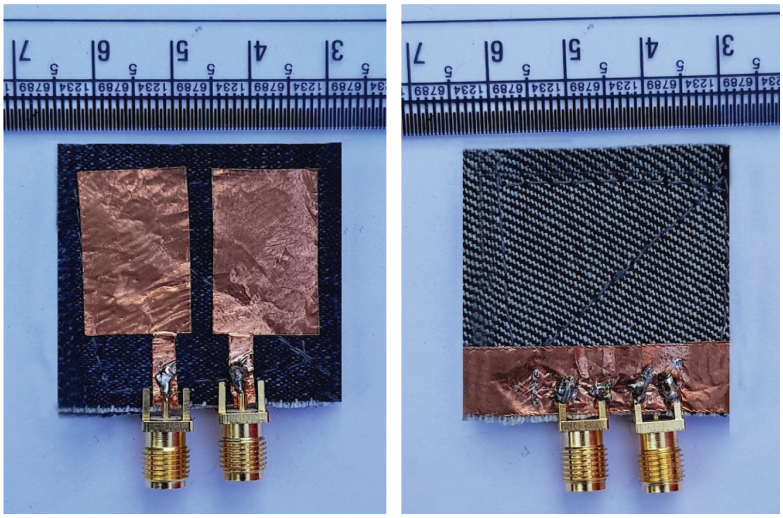

(a) (b)

Figure 5. Fabricated prototype of (a) upper portion of dual element MIMO configuration without isolator. (b) bottom portion of dual element MIMO configuration having partial ground plane and without isolator.

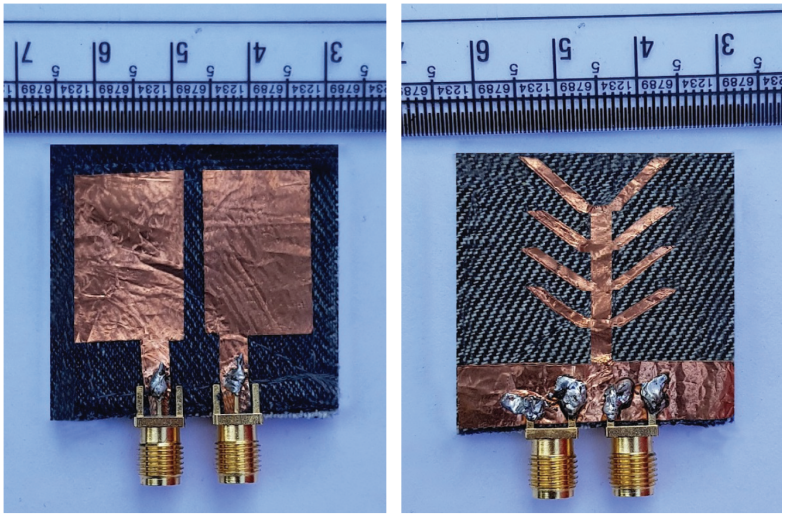

(a) (b)

Figure 6. Fabricated prototype of (a) upper portion of dual element MIMO configuration with isolator. (b) bottom portion of dual element MIMO configuration with a tree-shaped isolator connected to the partially etched ground plane.

2.1. Development of single antenna component

Before we reach our final design strategy, we systematically evaluate the single element model step by step. The rectangle shaped radiator was originally placed on the upper portion of jeans substrate with a single element. To obtain the broadband response to the antenna, the ground plane (GP) is configured. The Ansys HFSS[2] is used to model, optimize, and experimentally design the single component antenna. The dimension of the suggested antenna with one component is $35 \times 35 \times 1.59\ mm^3$, as evident from the Figures 1a and 1b. The simulation of antenna comprising of single rectangular component reveals the frequency spectrum from 1.45 to

[2]Ansys HF. Ansoft Corp., Pittsburgh, PA ver. 19.

Table 1. Dimensional constraints of the proposed UWB textile MIMO antenna.

Parameters	Values (in mm)	Parameters	Values (in mm)
W=L	35	L1	22.5
W1	7.5	L2	10
W2	14	L3	8.6
W3	3	L4	20.9
W4	13.5	L5	4.3
W5	7.2	L6	4.2
W6	10.9	L7	4.3
W7	10	L8	4.2
W8	16.5	g	3.2

12.02GHz (S11<-10dB). The fabricated model for the single component antenna is shown in the Figures 4a and 4b, respectively. The Anritsu VNA MS2037C (Anritsu Corporation, Atsugi, Japan) is used to test the developed model. The simulated outcome and the calculated S11 parameter of the manufactured antenna are depicted in Figure 7a. The calculated S11 (dB) has a frequency ranging from 1.21 to 12.13 GHz (S11<–10 dB). A strong affinity is achieved within the modeled and calculated tests. At the subsequent stage, a two-element MIMO antenna is built with two rectangular patch components, and the development technique is addressed in the following section.

2.2. MIMO antenna configuration with two components

The objective now is to build a MIMO antenna that matches the same UWB spectrum and has better antenna characteristics than a single rectangular element patch antenna. A dual element UWB MIMO antenna has also been built to cover the same UWB spectrum without changing its ground plane. The suggested prototype is designed and developed to evaluate experimentally. Figures 2a and 2b show the structure's top and bottom view, but Figure 2b is similar to the back view of Figure 1b. The fabricated prototype for the dual component UWB MIMO antenna without isolator is shown in Figures 5a and 5b, respectively. The antenna attains a frequency range operating from 1.96 to 12.46GHz (S11<–10 dB) through simulation. In addition, the MIMO antenna was tested using Anritsu VNA (Atsugi, Japan). Simulated and calculated S parameters are illustrated in Figure 7b. This design is consistent with the simulation results, spanning the measured frequencies from 1.57 to 12.22 GHz (for S11<-10 dB).

Nonetheless, if we examine MIMO characteristics from Figure 7b, it implies a very strong mutual coupling between the ports. Consequently, the current MIMO must include some high port isolation solution accompanying appropriate divergence parameters, such as channel capacity loss, diversity gain, envelope correlation coefficient, mean effective gain etc. With regard to this, the ground plane is only marginally changed by adding tree-shaped stub comprising of 8-branches. The following design methodology is addressed in Section 2.3.

2.3. Model of UWB MIMO antenna design with tree-shaped stub.

The UWB MIMO antenna is integrated with a tree-shaped stub comprising of 8-branches and attached to the ground plane to improve port isolation characteristics. The long size of the stub is $\lambda g/4$ (L4), where λg refers to the directed wavelength of lower UWB (3.1 GHz) frequency band.

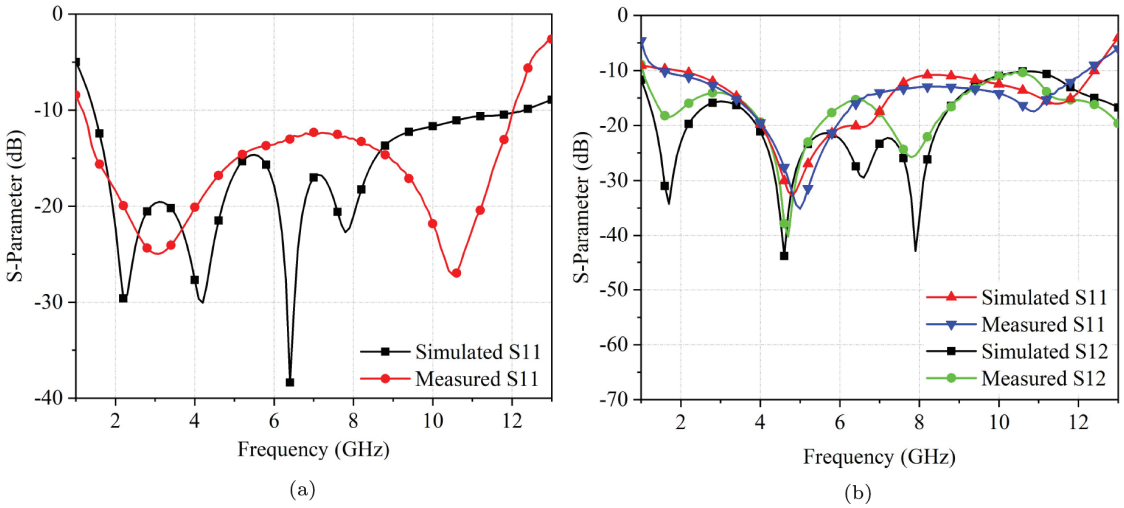

Figure 7. Simulated and measured outcomes for (a) single antenna element UWB antenna with partially etched ground (b) dual element UWB MIMO antenna with no isolator attached to ground plane.

The upper and bottom representation of the UWB MIMO antenna are depicted in the Figures 3a and 3b, whereas the fabricated prototype for the dual component UWB MIMO antenna with isolator is shown in Figures 6a and 6b, respectively. The model is simulated and tested experimentally. The results are favourable and are explained in the subsequent section.

3. Scattering parameters for the proposed design

The designed UWB MIMO antenna prototype was deployed with a tree-shaped stub comprising of -branches connected to the ground plane. The simulated and measured S-parameter(dB) characteristics indicate a very strong agreement with each other as depicted in Figure 8a. The analysis of S-parameters covers the frequency spectrum ranging from 1.71 to 12.63 GHz (simulation) and between 1.21 to 12.23 GHz (measurement) for S11 $<$-10dB.

From Figure 8a, it is inferred that measured and computed S12 are below –22 dB and –18dB, respectively throughout the whole UWB frequency band (3.1–10.6 GHz). The lowest isolation of 22 dB(measured) is at 9.23 GHz for the built-in UWB MIMO antenna, while the separation is higher across the device band at all the other frequencies. The insertion of stub improves port isolation by 43.19 dB (maximum) at 7.52 GHz. The comparisons help both parameters (S11 and S12) to acknowledge the simulation. A parametric analysis curve is also introduced in Figures 8b and 8c as a guidance for achieving isolation in between two ports.

Table 2 addresses the characteristics of the proposed UWB MIMO antenna. A minor difference is observed in results which is due to fabrication tolerances and some minor deficiencies with respect to the measurement tolerances.

Table 3 illustrates an assessment of the proposed model with some of the recently published articles on UWB MIMO antenna.

3.1. Characterization of envelope correlation coefficient (ECC) and diversity gain (DG)

The MIMO antenna's principal functional area is its diversity and multiplexing. For this reason, research on the diversity and performance of multiplexing is more important than isolation, reflection, and radiation [21]. The

Table 2. Summary of the proposed wearable UWB MIMO antenna characteristics.

Operating frequency (GHz)	S_{11} Simulated (dB)	S_{11} Measured (dB)	S_{12} Simulating (dB)	S_{12} Measured (dB)	Peak Rlz Gain Simulated (dB)	Peak Rlz Gain Measured (dB)
3.0	−15.47	−14.68	−22.82	−31.08	5.73	5.43
4.5	−14.69	−13.38	−37.33	−30.60	4.03	5.04
7.2	−20.30	−16.17	−26.20	−38.50	6.02	5.51
9.0	−16.93	−13.53	−25.20	−20.75	5.43	5.33
10.6	−13.95	−14.33	−32.81	−29.08	5.82	5.87

Table 3. Comparison with several recently reported UWB MIMO antenna articles.

Ref No.	Dimensions	elements	Dielectric, ϵ_r	Wearable	Max Gain	Element gap (mm)	Port Isolation (dB)
[3]	22 × 26	2	FR4, 4.4	No	3.8 dBi	6	>18
[6]	38.1 × 38.1	2	Substrate, 1.2	Yes	1.6 dBi	6.6	>20
[17]	25 × 30	2	FR4, 4.4	No	5.2 dBi	16	>20
[26]	50 × 30	2	FR4, 4.4	No	4.3 dB	Not Given	>20
[21]	45 × 25	2	FR4, 4.4	No	5.5 dB	10.4	>15
[29]	45 × 45	4	FR4, 4.4	No	4.9 dB	Not given	>17
proposed	35 × 35	2	Jeans, 2	Yes	5.88 dB	3.2	>22

envelope correlation coefficient(ECC) is a key element in assessing the performance of diversity in the MIMO antenna system.

In order to authenticate the capabilities of the suggested UWB MIMO antenna, it must be verified that the envelope correlation coefficient parameter is significantly very small, ideally below 0.5, suggesting the model built can provide a good margin of heterogeneity [3]. The intensity of the envelope correlation coefficient reflects the degree to which the communication channels are separated or linked. The envelope correlation coefficient calculation is based on the following Eq. 1 [21].

$$ECC = \frac{|S_{11}^{*}S_{12} + S_{21}^{*}S_{22}|}{(1 - |S_{11}|^2 - |S_{21}|^2)(1 - |S_{22}|^2 - |S_{12}|^2)} \tag{1}$$

The envelope correlation coefficient (ECC) curve of the suggested UWB MIMO antenna is determined with the help of S-parameters. Figure 8d shows the envelope correlation coefficient functionality of the UWB MIMO model. From the analysis, it can be inferred that the envelope correlation coefficient range is smaller than 0.012 over the whole UWB frequency spectrum.

The layout therefore encourages improved multiplexing quality through an increased data rate, which is very important for modern communication networks. The Diversity Gain(DG) is another parameter which should not be ignored during the design of MIMO antenna. In this article, the diversity gain is assessed with the following equation [12]

$$DG = 10\sqrt{1 - ECC^2} \tag{2}$$

The diversity gain for the suggested UWB MIMO antenna is anticipated from the envelope correlation coefficient equation which is shown in equation 2. The diversity gain of the suggested UWB MIMO model is illustrated in figure 8d. The figure illustrates that a very high diversity gain(value>9.9) is achieved from the proposed UWB MIMO antenna.

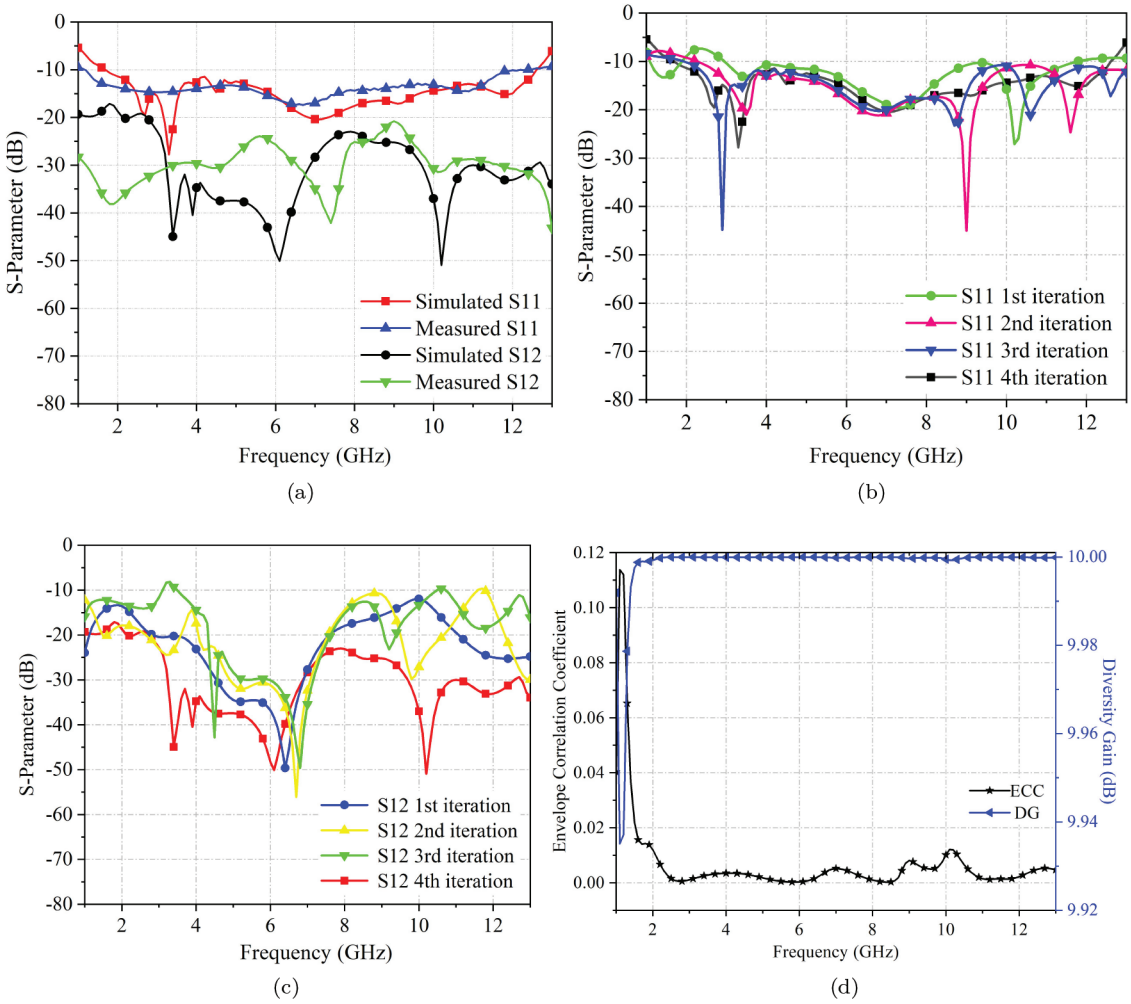

Figure 8. Simulated and measured outcomes for (a) dual element MIMO antenna with tree-shaped isolator attached to ground plane. (b) Parametric analysis of the UWB MIMO antenna(S11) (c) Parametric analysis of the UWB MIMO antenna(S12) (d) Envelope correlation coefficient and diversity gain of the UWB MIMO antenna with isolator.

3.2. Channel capacity loss and mean effective gain

Channel capacity loss (CCL) is another key factor in characterizing the capacity of the MIMO network. The channel capacity loss is responsible for the inter connection between the tightly spaced radiating components in a MIMO system. The channel capacity loss is determined using the following formula from S-parameters in a multipath system with a large signal-to-noise ratio. The channel capacity loss is evaluated from Eq. 3 [29]

$$CCL(loss) = -\log_2 det(\psi^R) \tag{3}$$

The ψ^R is a 2×2 correlation matrix where the matrix elements are obtained from the following equation, with respect to the Scattering parameters of the MIMO schema:

$$\psi_{ii} = 1 - (|S_{ii}|^2 + |S_{ij}|^2) \tag{4}$$

$$\psi_{ij} = 1 - (S_{ii}^* S_{ij} + S_{ji}^* S_{jj}) \tag{5}$$

where the terms i and j denote 1 and 2, respectively. Usually, a substantially small value of channel capacity loss is required for large channel strength. The minimum value of the MIMO antenna's channel capacity loss value is 0.4 (bit/s/Hz) [29]. Furthermore, the effects of channel capacity loss are modeled and graphically calculated in Figure 9a. From the graph, it can be inferred that the channel capacity loss value throughout the entire UWB band is found to be very low (CCL$<$0.27 bit/s/hz).

Thus, a nominal value of channel capacity loss in the communication channel with a high data rate transmits a highly successful information. This makes the aforesaid model for the UWB MIMO antenna suitable for mobile device applications.

Another important parameter corresponding to the characterization of MIMO antenna is the mean effective gain (MEG). The study of mean effective gain for the textile MIMO antenna is essential for analyzing its diversity characteristics in a wireless environment. It assists in understanding the gain parameter of the MIMO antenna. For attaining improved MIMO diversity performance, the deviation of the mean effective gain (MEG1-MEG2) relative to port 1 and port 2 should be less than ± 3 dB [17]. The mean effective gain parameter is evaluated according to the equation suggested in Eqs 6 and 7, respectively.

$$MEG1 = 0.5\eta_{1,rad} = [1 - |S_{11}|^2 - |S_{12}|^2] \tag{6}$$

$$MEG2 = 0.5\eta_{2,rad} = [1 - |S_{12}|^2 - |S_{22}|^2] \tag{7}$$

Figure 9a describes the mean effective gain difference (MEG1–MEG2), which is well below ± 0.14 dB, which provides a good diversity performance of the proposed MIMO antenna.

3.3. Total active reflection coefficient (TARC)

Total active reflection coefficient (TARC) is another important constraint to analyze MIMO antenna characteristics. Total active reflection coefficient consisted of all the valuable statistics relating to dispersion constraints for a multipurpose radiation system [11]. MIMO antenna's efficient impedance bandwidth, resonance conduct, and input excitation vector can be implemented by total active reflection coefficient. For a two-port antenna, it could be evaluated from Eqn 8 [11].

$$TARC = \frac{\sqrt{|S_{11} + S_{12}e^{j\theta}|^2 + |S_{21} + S_{22}e^{j\theta}|^2}}{\sqrt{2}} \tag{8}$$

Where the term θ represents the angular excitation phase at the port of excitation, which is swept from 0 to 180°. S_{11} and S_{22} represents the reflection coefficients of the two input ports and S_{12} and S_{21} represents the port isolation.

The resonance properties of the proposed antenna are scrutinized via nabbing a few of the excitation phase's randomly selected angles. The total active reflection coefficient curve of the proposed MIMO antenna

design is illustrated in Figure 9b. The suggested wearable UWB MIMO antenna is typically attached to the humanoid or to other animal in motion. Hence, the input signal phase angle can, therefore, vary at variable positions.

We consider 9 variable angles of the phase for excitation viz $30°, 60°, 90°, 120°, 150°, 120°, and 180°$, respectively. Figure 9b shows that, for the whole series of phase angles, the total active reflection coefficient curve offers a constant resonance and impedance bandwidth. There are no significant losses in antenna efficiency after the antenna is attached to the moving human physique.

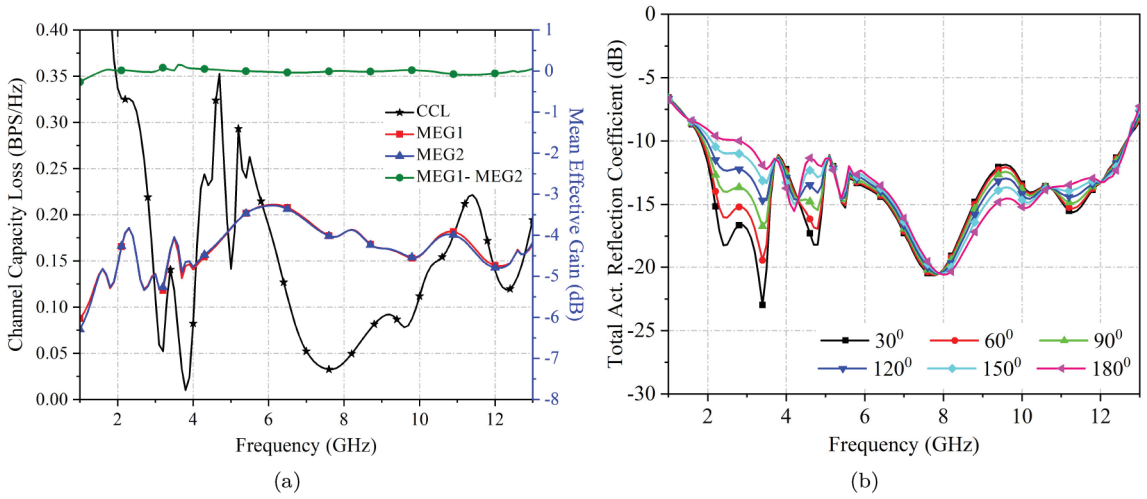

Figure 9. Representation of (a) Channel capacity loss and mean effective gain of the proposed UWB MIMO antenna with isolator. (b) Total active reflection coefficient of the proposed UWB MIMO antenna with isolator.

3.4. Surface current distributions

The surface current distribution of the proposed MIMO antenna is also examined. This investigation is required in order to understand the reduction in the coupling between the number of ports. The Figures 10 a–10d show the latest GP stub-born and stub-less distributions. We have also studied the existing dispersion within the service band at four different frequencies. It is noted that when the tree-shaped stub is incorporated into the design, the current flowing from input spanning port 1 to port 2 is very insignificant or weak; it contributes to very limited mutual coupling in between the two rectangle shaped antenna components.

Proper stub positioning includes stop band features, which decreases the transfer of the current from one terminal to the other terminal. It allows to incorporate the second radiating element a lower current in order to realize high port decoupling with the first radiator [17]. The surface current representation at 2.4, 3.5, 5.8, and 8 GHz for both the MIMO antennas with and without tree shaped stub are represented in Figurea 10a–10d, respectively.

3.5. MIMO antenna radiation pattern

We have also tested the quality of the radiation of the UWB MIMO textile antenna in the E-plane and H-plane. Here, the standard 2D radiation patterns of the simulated and measured prototypes at 2.4, 3.5, 5.8, and 7.5 GHz are shown in Figure 11a–11d.

The antenna provides bidirectional radiation at 2.4 and 3.5GHz, whereas it provides unidirectional radiation pattern at 5.8 and 7.5 GHz for the E-plane and provides monopole like radiation pattern for H-plane. The calculated and simulated radiation levels indicate that they are well coordinated.

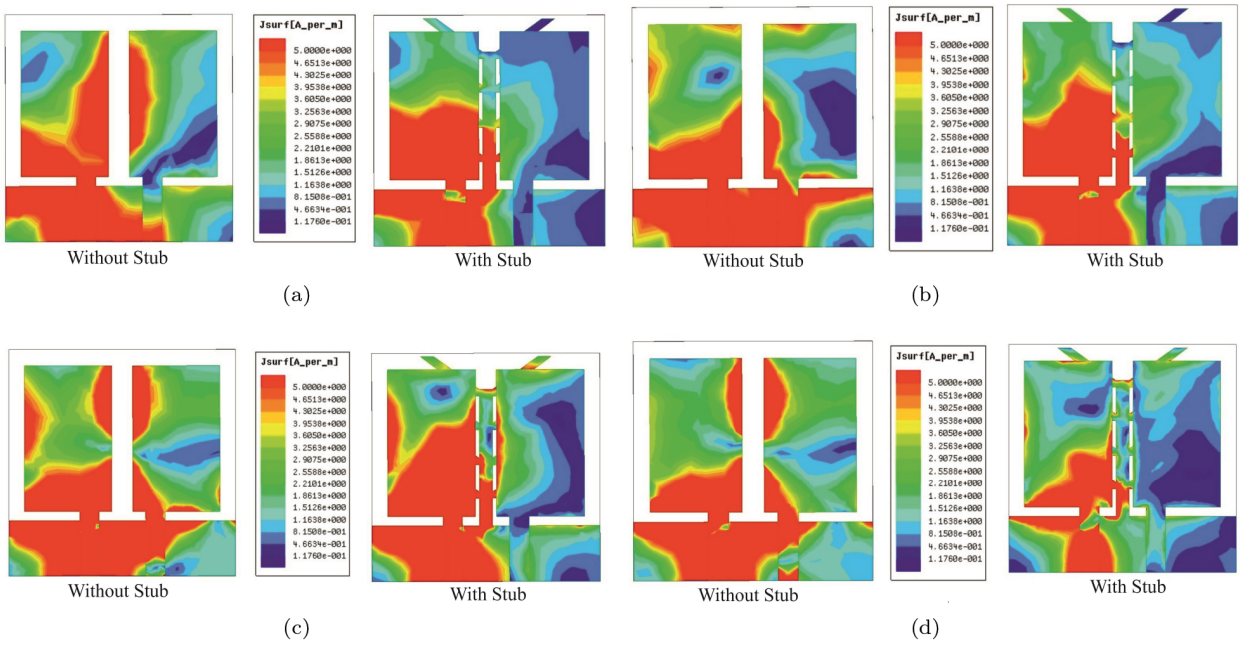

Figure 10. Surface current distribution of the MIMO antenna for (a) 2.4GHz (b) 3.5GHz (c) 5.8GHz (d) 8GHz.

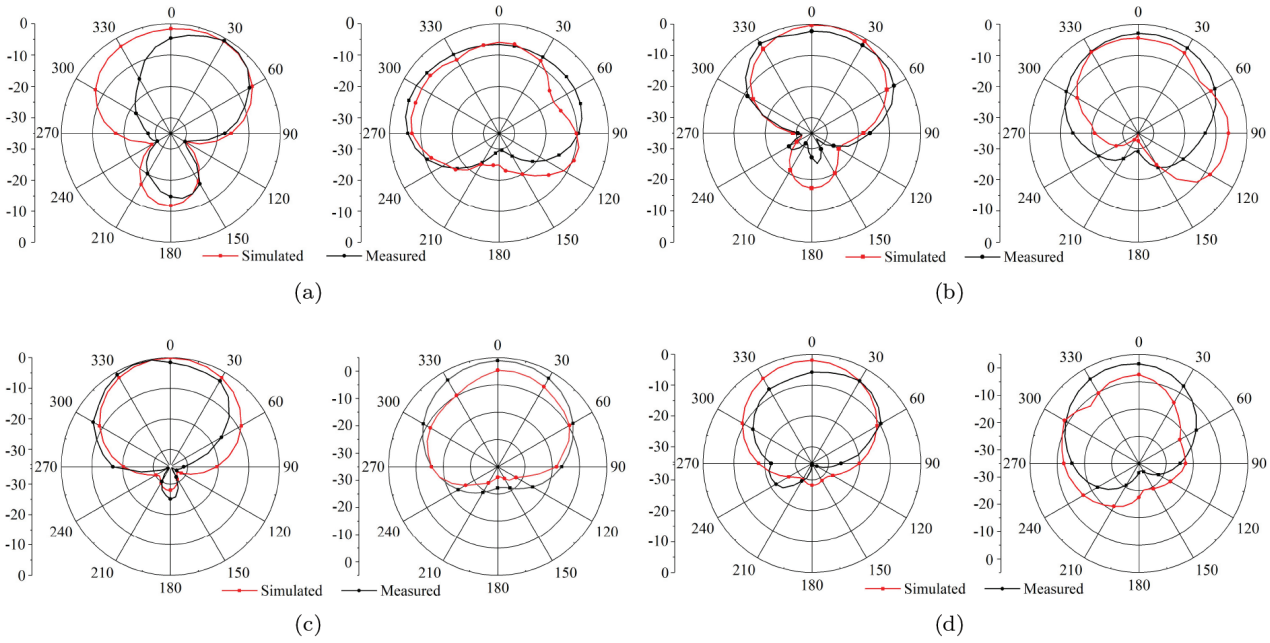

Figure 11. Simulated and measured radiation patterns of the UWB MIMO antenna for frequencies operating at (a) 2.4GHz (b) 3.5GHz (c) 5.8GHz (d) 7.5GHz.

3.6. Impacts on the S-parameters of the proposed UWB MIMO antenna on-body attachment

To register the influence of radiation and to check its impact on the human body a prototype for the human tissue model is simulated and reflected in Figure 12a. Table 4 represents the prospective properties of tissue model at 2.4GHz.

The tissue model comprises of a multilayered segment of skin, muscle, and body fat on a skeletal structure. All of this pertains to the tissue model to have its own unique features like thickness, permittivity factor, mass density along with its conductivity.

Table 4. The material properties assigned to the human tissue phantom at 2.4GHz.

Layers	ϵ_r	σ (S/m)	Density (kg/m^3)	Thickness (mm)
Skin	37.95	1.49	1001	2
Fat	5.27	0.11	900	5
Muscle	52.67	1.77	1006	20
Bone	18.49	0.82	1008	13

The properties of human tissue model are sourced from the Ansys HFSS reference library[3], and the S-parameters of the designed prototype have been examined. Furthermore, to test the impact of antenna on body conditions, the antenna is worn by an individual separately at the wrist and the shoulder and used the VNA to measure the S-parameters. Such observations were compared to the outcomes for off-body tests, which is illustrated in Figures 12b and 12c, respectively. The suggested antenna design covered the entire UWB spectrum in all situations. The modeled and measured gain is shown in the Figure 12d and illustrated with slight deviation between them, which might be due to fabrication tolerances. The maximum antenna gain (measured) in the operating UWB frequency spectra is around 5.88 dB at 6.4 GHz.

From the graph it is inferred that the proposed low-profile textile UWB MIMO antenna not only provides good mobile functionality, rather it also has UWB features of extremely high port isolation over the entire band (port isolation $>$ 22 dB), which is the innovation and novelty of the proposed work. We found that, in all cases, the proposed antenna provides full operating bands of WIMAX (3.2–3.8 GHz), wireless LAN (5.15–5.35/5.72–5.85GHz), uplink C bands (3.7–4.2/5.9–6.425GHz), ITU (8-8.5GHz) band, and downlink (7.2–7.7GHz) defense bands. We found no significant incoherence in the behavior of the antenna.

4. Conclusion

This article addresses and describes a dual element portable UWB MIMO antenna for wearable applications. The integration of tree-shaped stub into the ground plane of the structure leads to high decoupling of ports. It has covered 1.21 to 12.23GHz measured bandwidth that complies with the bandwidth of WiMAX (3.2–3.8GHz), wireless local area network (5.15–5.35/5.72–5.85GHz), downlink-uplink C band (3.7–4.2/5.9–6.425GHz), defense downlink (7.2–7.7GHz), ITU(8-8.5GHz), and almost all UWB-band applications (3.1-10.6GHz). The port isolation of more than 22 dB is achieved throughout the application band. The research's unique feature is that port isolation is achieved with a component spacing of just 3.2mm. The MIMO antenna proposed offers highly nominal envelope correlation coefficient (value $<$ 0.012) and channel capacity loss (value $<$ 0.27 BPS/Hz). The higher diversity gain (value $>$ 9.9) and the mean effective gain (value $\pm$ 0.14) ratio confirm that the research

[3]Ansys HF. Ansoft Corp., Pittsburgh, PA ver. 19.

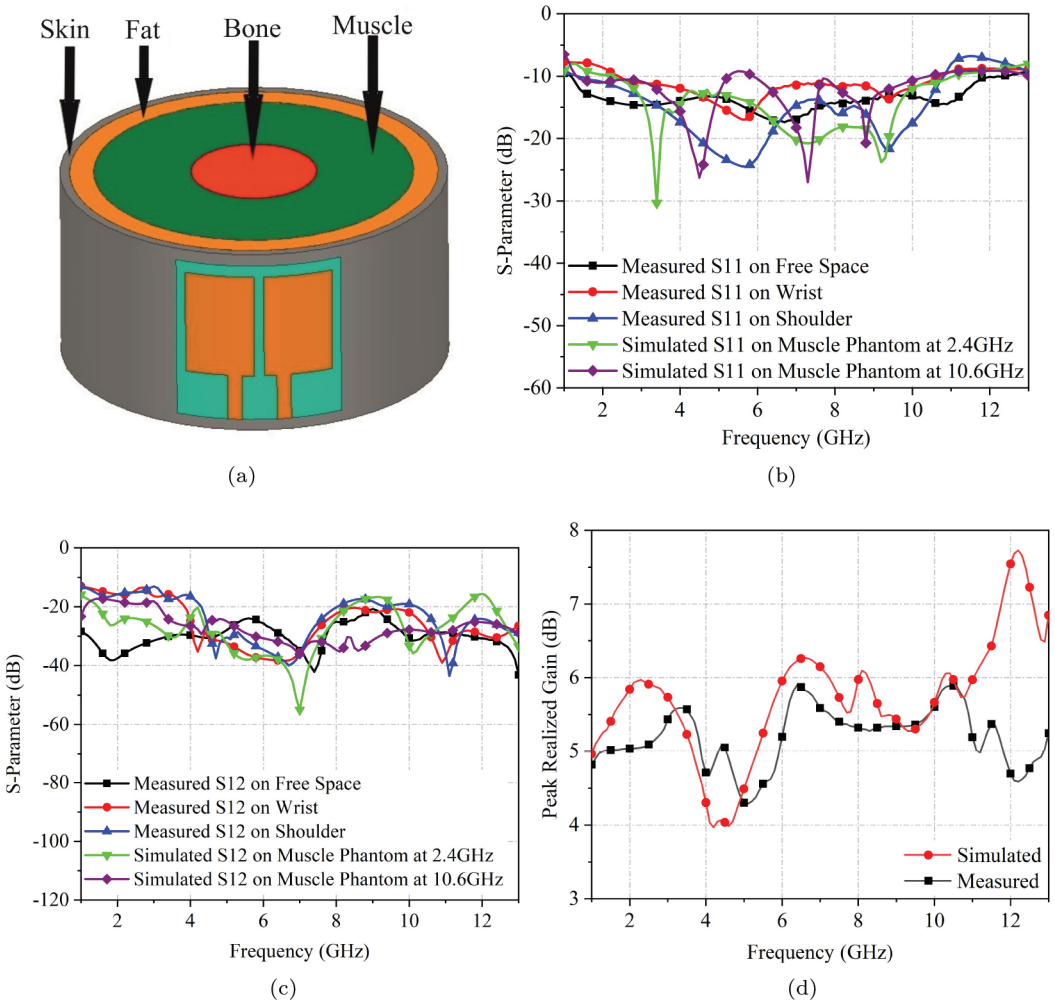

Figure 12. Representation of (a) Proposed UWB MIMO antenna attached to human phantom model comprising of different layers (b) Comparison of simulated and measured S11 on different occasions. (c) Comparison illustrating simulated and measured S12 on different occasions. (d) Simulated and measured peak realized gain of the UWB MIMO antenna.

into the design of MIMO antenna is successful. The calculated results are consistent with the modeled outcomes. In addition, the bodily measurement indicates that the antenna structure offers the full UWB bandwidth to the off-body situation.

References

[1] Yan S, Vandenbosch GA. Radiation pattern-reconfigurable wearable antenna based on metamaterial structure. IEEE Antennas and wireless propagation Letters 2016; 15: 1715-1718. doi: 10.1109/LAWP.2016.2528299

[2] Panda AK, Sahu S, Mishra RK. A compact dual-band 2 x 1 metamaterial inspired mimo antenna system with high port isolation for LTE and WiMax applications. International Journal of RF and Microwave Computer-Aided Engineering 2017; 27(8): e21122. doi: 10.1002/mmce.21122.

[3] Luo CM, Hong JS, Zhong LL. Isolation enhancement of a very compact UWB-MIMO slot antenna with two defected ground structures. IEEE Antennas and Wireless Propagation Letters 2015; 14: 1766-1769. doi: 10.1109/LAWP.2015.2423318.

[4] Shakib MN, Moghavvemi M, Mahadi WN. Design of a tri-band off-body antenna for WBAN communication. IEEE Antennas and Wireless Propagation Letters 2016; 16: 210-213. doi: 10.1109/LAWP.2016.2569819.

[5] Hu B, Gao GP, He LL, Cong XD, Zhao JN. Bending and on-arm effects on a wearable antenna for 2.45 GHz body area network. IEEE Antennas and Wireless Propagation Letters 2015; 15: 378-381. doi: 10.1109/LAWP.2015.2446512.

[6] Li H, Sun S, Wang B, Wu F. Design of compact single-layer textile MIMO antenna for wearable applications. IEEE Transactions on Antennas and Propagation 2018; 66(6): 3136-3141. doi: 10.1109/TAP.2018.2811844.

[7] Yan S, Soh PJ, Vandenbosch GA. Dual-band textile MIMO antenna based on substrate-integrated waveguide (SIW) technology. IEEE Transactions on Antennas and Propagation 2015; 63(11): 4640-4647. doi: 10.1109/TAP.2015.2477094.

[8] Mendes C, Peixeiro C. A dual-mode single-band wearable microstrip antenna for body area networks. IEEE Antennas and Wireless Propagation Letters 2017; 16: 3055-3058. doi: 10.1109/LAWP.2017.2760142.

[9] Zhu XQ, Guo YX, Wu W. A compact dual-band antenna for wireless body-area network applications. IEEE Antennas and Wireless Propagation Letters 2015; 15: 98-101. doi: 10.1109/LAWP.2015.2431822.

[10] Shakib MN, Moghavvemi M, Mahadi WN. Design of a tri-band off-body antenna for WBAN communication. IEEE Antennas and Wireless Propagation Letters 2016; 16: 210-213. doi: 10.1109/LAWP.2016.2569819.

[11] Sharawi MS. Printed MIMO Antenna Engineering. Norwood, Massachusetts, MA, USA: Artech House; 2014.

[12] Iqbal A, Basir A, Smida A, Mallat NK, Elfergani I et al. Electromagnetic bandgap backed millimeter-wave MIMO antenna for wearable applications. IEEE Access 2019; 7: 111135-111144. doi: 10.1109/ACCESS.2019.2933913.

[13] Singh N, Singh AK, Singh VK. Design & performance of wearable ultra wide band textile antenna for medical applications. Open Engineering 2015; 57: 1553–1557. doi: 10.1002/mop.29131.

[14] Ramachandran A, Mathew S, Rajan V, Kesavath V. A compact triband quad-element MIMO antenna using SRR ring for high isolation. IEEE Antennas and Wireless Propagation Letters 2016; 16: 1409-1412. doi: 10.1109/LAWP.2016.2640305.

[15] Malathi AC, Thiripurasundari D. Review on isolation techniques in MIMO antenna systems. Indian Journal of Science and Technology 2016; 9(35): 1-10. doi: 10.17485/ijst/2016/v9i35/96704.

[16] Ghosh S, Tran TN, Le-Ngoc T. Dual-layer EBG-based miniaturized multi-element antenna for MIMO systems. IEEE Transactions on Antennas and Propagation 2014; 62(8): 3985-3997. doi: 10.1109/TAP.2014.2323410.

[17] Roshna TK, Deepak U, Sajitha VR, Vasudevan K, Mohanan P. A compact UWB MIMO antenna with reflector to enhance isolation. IEEE transactions on Antennas and Propagation 2015; 63(4): 1873-18777. doi: 10.1109/TAP.2015.2398455.

[18] Abdalla MA, Ibrahim AA. Compact and closely spaced metamaterial MIMO antenna with high isolation for wireless applications. IEEE Antennas and Wireless Propagation Letters 2013; 12:1452-1455. doi: 10.1109/LAWP.2013.2288338.

[19] Zhai G, Chen ZN, Qing X. Enhanced isolation of a closely spaced four-element MIMO antenna system using metamaterial mushroom. IEEE Transactions on Antennas and Propagation 2015; 63(8): 3362-3370. doi: 10.1109/TAP.2015.2434403.

[20] Iqbal A, Saraereh OA, Ahmad AW, Bashir S. Mutual coupling reduction using F-shaped stubs in UWB-MIMO antenna. IEEE Access 2017; 6: 2755-2759. doi: 10.1109/ACCESS.2017.2785232.

[21] Mathur R, Dwari S. Compact CPW-Fed ultrawideband MIMO antenna using hexagonal ring monopole antenna elements. AEU-International Journal of Electronics and Communications 2018; 93: 1-6. doi: 10.1016/j.aeue.2018.05.032.

[22] Bardera EC, Sánchez-Fernandez M, Talegon LA, Delgado AV. Feasibility of a wearable textile antenna hub based on massive MIMO systems. In: 2016 18th Mediterranean Electrotechnical Conference (MELECON) 2016; 1-6. doi: 10.1109/MELCON.2016.7495384.

[23] Chen HN, Song JM, Park JD. A compact circularly polarized MIMO dielectric resonator antenna over electromagnetic band-Gap surface for 5G applications. IEEE Access 2019; 7: 140889-140898. doi: 10.1109/ACCESS.2019.2943880.

[24] Saleem R, Bilal M, Bajwa KB, Shafique MF. Eight-element UWB-MIMO array with three distinct isolation mechanisms. Electronics Letters 2015; 51(4): 311-313. doi: 10.1049/el.2014.4199.

[25] Ouyang Y, Love DJ, Chappell WJ. Body-worn distributed MIMO system. IEEE Transactions on Vehicular Technology 2008; 58(4): 1752-1765. doi: 10.1109/TVT.2008.2004491.

[26] Zhu L, Hwang HS, Ren E, Yang G. High performance MIMO antenna for 5G wearable devices. In2017 IEEE International Symposium on Antennas and Propagation & USNC/URSI National Radio Science Meeting 2017; 1869-1870. doi: 10.1109/APUSNCURSINRSM.2017.8072977.

[27] Qu L, Piao H, Qu Y, Kim HH, Kim H. Circularly polarised MIMO ground radiation antennas for wearable devices. Electronics Letters 2018; 54(4): 189-190. doi: 10.1049/el.2017.4348.

[28] Sankaralingam S, Gupta B. Determination of dielectric constant of fabric materials and their use as substrates for design and development of antennas for wearable applications. IEEE Transactions on Instrumentation and Measurement 2010; 59(12): 3122-3130. doi: 10.1109/TIM.2010.2063090.

[29] Tripathi S, Mohan A, Yadav S. A compact Koch fractal UWB MIMO antenna with WLAN band-rejection. IEEE Antennas and wireless propagation letters 2015; 14: 1565-1568. doi: 10.1109/LAWP.2015.2412659.